Surface Modification of Polycarbonate by Radio-Frequency Plasma and Optimization of the Process Variables with Response Surface Methodology

N. Gomathi,[1] C. Eswaraiah,[2] Sudarsan Neogi[1]

[1]*Department of Chemical Engineering, Indian Institute of Technology, Kharagpur 721302, India*
[2]*Mineral Processing Department, Institute of Minerals and Materials Technology, Bhubaneswar 751013, India*

Received 6 February 2009; accepted 26 April 2009
DOI 10.1002/app.30691
Published online 23 June 2009 in Wiley InterScience (www.interscience.wiley.com).

ABSTRACT: This study deals with the radio-frequency plasma treatment of polycarbonate surfaces with argon. The wettability of polycarbonate was examined by static contact angle measurements with polar solvents (deionized water and formamide) and a nonpolar solvent (diiodomethane). The surface free energy of the polycarbonate obtained from the measured contact angle demonstrated that exposure to argon plasma resulted in an increased surface energy and polarity compared to the untreated polycarbonate. Attenuated total reflection/Fourier transform infrared spectroscopy indicated that argon plasma treatment resulted in surface chemistry changes by hydrogen abstraction from the phenyl ring and methyl group and chain scission at the ether and carbonyl sites. These led to the formation of hydroxyl groups and double bonds. With scanning electron microscopy and atomic force microscopy analysis, changes in the surface morphology and roughness before and after plasma treatment were observed. We followed an experimental matrix with the identified process variables affecting the wettability of the polymer, and optimized the experiments with the response surface methodology of a central composite design. A quadratic model was developed to represent the surface energy in terms of process variables. Optimized process conditions were derived from the predicted model and were confirmed by the experimental data at the predicted optimum conditions. The prediction accuracy of the model was found to be very high. © 2009 Wiley Periodicals, Inc. J Appl Polym Sci 114: 1557–1566, 2009

Key words: atomic force microscopy (AFM); FT-IR; polycarbonates

INTRODUCTION

Polycarbonates, which are long-chain linear polyesters of carbonic acid and dihydric phenols, have a broad range of applications for automobile headlamps, corrective lenses, compact discs, syringes, and medical devices. Despite the advantages of polycarbonate, such as its transparency and toughness, it has a low surface energy, which leads to poor adhesion.[1] The increasing demand for desirable surface functional properties, such as wettability, friction factor, adhesivity, printability, and biocompatibilty, has led to the development of various surface modification methods designed to preserve the bulk properties. Among the various methods, plasma surface modification, which is limited to a depth of 50 Å to 10 μm, is important in improving the hydrophilicity of polymeric substrates by inducing physical and chemical changes on the surface without influencing the bulk properties. It is even possible to treat an inert surface of any geometry by this method. It is a clean technique because it does not require any chemicals or solvents. The main benefits of plasma surface modification that have been reported are surface cleaning, ablation, crosslinking, and modification of the surface chemical structure.[2] Depending on the gas used, plasma causes the chain scission of existing groups and creates new functional groups, such as —OH, —OOH, and —NH_2. The surface of the polymers can be tuned to tailor-make the polymers for specific end use by proper selection of the plasma gases. For example, the hydrophilicity of a polymer surface can be improved by its treatment with oxygen-containing plasmas (oxygen plasma, H_2O plasma, or CO_2 plasma), whereas it can be made hydrophobic by the use of fluorine-containing plasma.[3–6]

Plasma surface cleaning, especially that with argon plasma, can improve the surface adhesion by the removal of surface contaminants and weakly bonded molecular layers by sputtering.[7] It has been reported that, during plasma treatment with noble gases, the crosslinking of the polymer surface is dominant, and this improves the adhesion properties of polymers.[8,9] Among the various active species,

Correspondence to: S. Neogi (sneogi@che.iitkgp.ernet.in).
Contract grant sponsor: Department of Science and Technology (New Delhi, India).

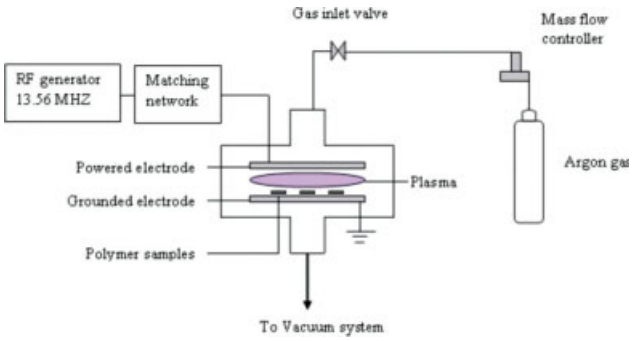

Figure 1 Experimental setup. [Color figure can be viewed in the online issue, which is available at www.interscience.wiley.com.]

such as free radicals, electrons, ions, metastable species, and photons, free radicals and electrons collide with the material surface, rupture the covalent bonds, and leave the free radicals on the surface. These free radicals then combine with oxygen or moisture in air when they are exposed to the atmosphere.[10]

Radio-frequency (RF) plasma (13.56 MHz) treatment was used in this study to modify the surface of polycarbonate to improve its wettability. The objective was to develop an empirical model of the process and to make a more precise assessment of the optimum operating conditions for the governing factors. Conventional methods of optimizing the process conditions involve the optimization of one variable at a time with the other variables kept constant. This may lead to misinterpretation of results because the interactions among the factors are not taken into account.[11] With the design of experiments, the relationship between the process variables and the response is established.[12,13] Response surface methodology (RSM), which is applicable for a maximum of five variables, was used in this study to optimize the process conditions to maximize the wettability of the polycarbonate. The effects of plasma treatment on the surface chemistry and surface morphology of the polycarbonate were studied in detail.

EXPERIMENTAL

RF plasma treatment

The polycarbonate sheets used in this study were food grade and were procured from M/s Plastic Abhiyanta (Kolkata, India). These were cut into small pieces that were $2'' \times 1''$ and were cleaned in an ultrasonic cleaner for 10 min with isopropyl alcohol. The argon plasma treatment of the polycarbonate was carried out with a plasma reactor M-PECVD-1A[S] (Milman Thin Film Systems, Pune, India). A schematic diagram of the PECVD reactor used in this study is shown in Figure 1. The main components of the reactor were a pumping system, a reactor chamber, a gas feed system, and an RF power source. The pumping system was composed of rotary and roots pumps, which helped to evacuate the reactor chamber down to a pressure under 0.1 Pa before the plasma treatment. In the reactor chamber, the top-powered electrode plate had perforations to provide a uniform distribution of gas, through which argon gas was supplied. The downgrounded electrode plate accommodated the interchangeable substrate holder, on which the polymer samples were placed. Argon gas was introduced through a mass flow controller at a specified flow rate. The process pressure was maintained by a closed-loop pressure control system. The plasma excitation was obtained by a 13.56-MHz RF generator provided with a matching network. The matching network helped to maintain zero reflected power so that the incident power was same as the plasma power. The experiments were run at various conditions to study the effects of process variables such as power, pressure, flow rate, and time on the wettability, surface chemistry, and surface morphology. The treated samples were stored separately in sealed plastic bags. The samples were characterized after 2 months of aging by various techniques to study the changes caused by plasma.

Contact-angle measurement

The energy of a surface is directly related to its wettability, which is measured by the contact angle. In contact angle measurement, a liquid drop is placed onto a solid surface. Whether it sits on the surface in the form of a droplet or spreads out over the surface depends on the interfacial free energies of the two substances. Static contact angle measurements were carried out by the sessile drop method with a Rame-Hart 500-F1 advanced goniometer (Rame-Hart Instrument Co., Netcong, NJ) at ambient humidity and temperature with two different polar liquids (deionized water and formamide) and one nonpolar liquid (diiodomethane). The static contact angles were measured on at least five different locations of the polycarbonate surface, as shown in Figure 2, and

Figure 2 Drop positions in contact-angle measurements.

the average values for the contact angles were calculated. The total surface energy (γ_s) was calculated as the sum of the polar component (γ_s^p) and dispersive component (γ_s^d) according to the Fowkes approximation, and the surface polarity was estimated as the ratio of γ_s^p to γ_s.[15,16]

Surface chemistry

Fourier transform infrared (FTIR) spectroscopy was used for to investigate the changes in the chemical structure of polycarbonate. Because the plasma surface modification was confined to a few molecular layers of the surface, the extent of the surface reaction was monitored with infrared spectra in the attenuated total reflection (ATR) mode. FTIR measurements, including 32 scans, were performed on a ThermoNicolet Nexus 870 FTIR (Thermo Nicolet Corp., North America, Madison, WI) in the range 4000–600 cm^{-1} with a resolution of 4 cm^{-1}.

Surface morphology

The morphology of the samples was observed by scanning electron microscopy (SEM; JSM-5800, JEOL, Tokyo, Japan). The samples were coated with a thin conductive layer of gold under vacuum conditions before analysis. The surface topography and roughness of the polycarbonate before and after plasma treatment were analyzed by atomic force microscopy (AFM). Topographical and roughness characterizations were performed by AFM with an SPM1000 scanning probe microscope from Nanonics (Israel). Intermittent mode was used for the scanning range of 10.0 × 10.0 μm^2 at a scan rate of 8 ms/point. The samples were scanned with a glass fiber tip with a tip diameter of 20 nm. All samples were scanned at room temperature in the atmosphere. The root-mean-square roughness was determined with WSxM 4 Develop 11.4 software (Nanotec Electronica SL, Spain).

Experimental design and optimization model

The process variables that influence the effect of plasma include power, total pressure in the reactor chamber, flow rates of various gases, treatment time, materials of the electrodes and their distance, substrate temperature, and reactor geometry.[17] Zajickova et al.[7] studied the effect of the treatment time, gas flow rate, and pressure on the surface free energy. They studied the improved adhesion by depositing organosilicon thin films on the untreated and plasma-treated polycarbonate. Carrino and coworkers[18,19] selected voltage, air flow rate, and treatment time as process variables and studied their effects on the wettability and aging time of wettability on the surface of polypropylene. The selection of variables was done with the help of the previously mentioned articles and preliminary experimental studies. The variables and their range, presented in Table I, were selected in such a way to cover all possible experimental conditions.

TABLE I
Levels and Ranges of the Variables Used in the Experimental Design

	Range and level				
Variable	−2	−1	0	1	2
Power (W)	20	65	110	155	200
Pressure (mTorr)	100	125	150	175	200
Flow rate (sccm)	5	10	15	20	25
Time (min)	2	4	6	8	10

RSM is an integration of mathematical and statistical technique and is used to design experiments, develop models, evaluate the effects of factors, and optimize factors for the desired response. It is used to improve existing product designs apart from the design, development, and formulation of new products. Central composite design, the most used response surface method, was performed with four variables at five levels to show the statistical significance of the effect of the process variables on the response. The RF power, pressure, flow rate of argon gas, and plasma treatment time were considered independent process variables. The surface energy of the polymer was taken as the dependent response variable.

Thirty experiments with 16 cube points and eight star points with six replications at the center points were performed (Table II). An axial distance of 2 was chosen to make this design rotated. The following quadratic polynomial equation was used to predict the response as a function of the independent process variables and their interaction.[20]

$$Y = \beta_0 + \sum_{i=1}^{4} \beta_i X_i + \sum_{i=1}^{4} \beta_{ii} X_i^2 + \sum_{i=1}^{4} \sum_{j=i+1}^{4} \beta_{ij} X_i X_j + e \quad (1)$$

where Y is the response; β_0 is the constant coefficient; X_i and X_j (i and j = 1–4) are noncoded variables; β_i, β_{ii}, and β_{ij} (i and j = 1–4) are linear, quadratic, and second-order interaction coefficients, respectively; and e is the error function. The variance of each experimental factor was divided into linear, quadratic, and interaction variances to assess the adequacy of the second-order polynomial function and the significance of the terms. The coefficients of the model were estimated with multiple-regression analysis. The fit of the model was judged from the coefficients of correlation and regression.

The fit adequacy of the second-order polynomial equation was expressed by the coefficient of determination (R^2). The R^2 value indicates how much

TABLE II
Full Factorial Central Composite Design for the Surface Energy of Polycarbonate

Sample	Power (W)	Pressure (mTorr)	Flow rate (sccm)	Time (min)	γ_s^p (mN/m)	γ_s^d (mN/m)	Surface polarity[a]	γ_s (mN/m)
1	65	125	10	4	6.27	31.33	0.167	37.60
2	155	125	10	4	6.01	29.41	0.170	35.43
3	65	175	10	4	3.48	38.22	0.084	41.71
4	155	175	10	4	3.65	35.94	0.092	39.60
5	65	125	20	4	7.73	30.14	0.204	37.87
6	155	125	20	4	3.82	33.36	0.103	37.18
7	65	175	20	4	12.47	28.37	0.305	40.84
8	155	175	20	4	6.87	31.95	0.177	38.82
9	65	125	10	8	5.12	34.13	0.130	39.25
10	155	125	10	8	4.76	30.29	0.136	35.05
11	65	175	10	8	7.57	33.42	0.185	41.00
12	155	175	10	8	3.73	33.72	0.100	37.45
13	65	125	20	8	6.82	32.62	0.173	39.43
14	155	125	20	8	4.37	32.18	0.120	36.56
15	65	175	20	8	4.44	36.39	0.109	40.83
16	155	175	20	8	5.26	33.61	0.135	38.88
17	20	150	15	6	6.31	34.47	0.155	40.78
18	200	150	15	6	4.82	31.45	0.133	36.28
19	110	100	15	6	4.56	29.36	0.135	33.92
20	110	200	15	6	8.14	32.56	0.200	40.70
21	110	150	5	6	4.45	33.04	0.119	37.49
22	110	150	25	6	4.81	33.89	0.124	38.69
23	110	150	15	2	7.13	32.40	0.180	39.53
24	110	150	15	10	5.41	34.44	0.136	39.85
25	110	150	15	6	4.01	35.08	0.102	39.09
26	110	150	15	6	9.83	29.97	0.247	39.80
27	110	150	15	6	7.79	30.06	0.206	37.85
28	110	150	15	6	7.41	30.65	0.195	38.06
29	110	150	15	6	5.69	34.07	0.143	39.76
30	110	150	15	6	6.34	33.00	0.161	39.34

[a] $\gamma_s^p/(\gamma_s^p + \gamma_s^d)$.

variability in the observed response values can be explained by the experimental factors and their interactions. When R^2 approaches unity, the empirical model fits the actual data.[20]

Data were processed by eq. (1) with the Design-Expert 7.1.4 (trial version, Stat-Ease, Inc., Minneapolis, MN) program, including an analysis of variance (ANOVA) to obtain the effect of the process variables on the response. The quality of the fit of the polynomial model was expressed by R^2, and its statistical significance was checked by the F test.[11] The significance of the regression coefficient was tested by a t test. A probability (P) value of 0.05 was set before we assessed the statistical significance of the estimates.

RESULTS AND DISCUSSION

Contact angle measurement

The results of the contact angle measurements of the argon-plasma-treated polycarbonate under various process conditions are presented in Table II. The untreated polycarbonate exhibited contact angles of 89.48, 69.75, and 49.875° with deionized water, formamide, and diiodomethane, respectively, and were reduced after plasma treatment. The plasma treatment increased γ_s of polycarbonate (untreated polycarbonate: $\gamma_s = 33.112$ mN/m, $\gamma_s^p = 1.28$ mN/m, and $\gamma_s^d = 31.83$ mN/m) by increasing γ_s^p. In all of the plasma-treated samples, the lower values of the contact angles (not shown) explained their higher surface energy, which provided a measure of their hydrophilicity. The bombardment by plasma species created free radicals on the polymer surface mainly by chain scission/hydrogen abstraction, which subsequently combined with oxygen from air to increase the polarity.[16,21,22] Despite the increased polar components, longer exposure times did not cause significant changes in the surface energy but resulted in increased surface roughness. It was reported that the surface chemistry and surface morphology affect the contact angle of the polymer surface.[23–25] The significant increase in the polarity of the plasma-treated polycarbonate, presented in Table II, clearly indicated the incorporation of new functional groups.

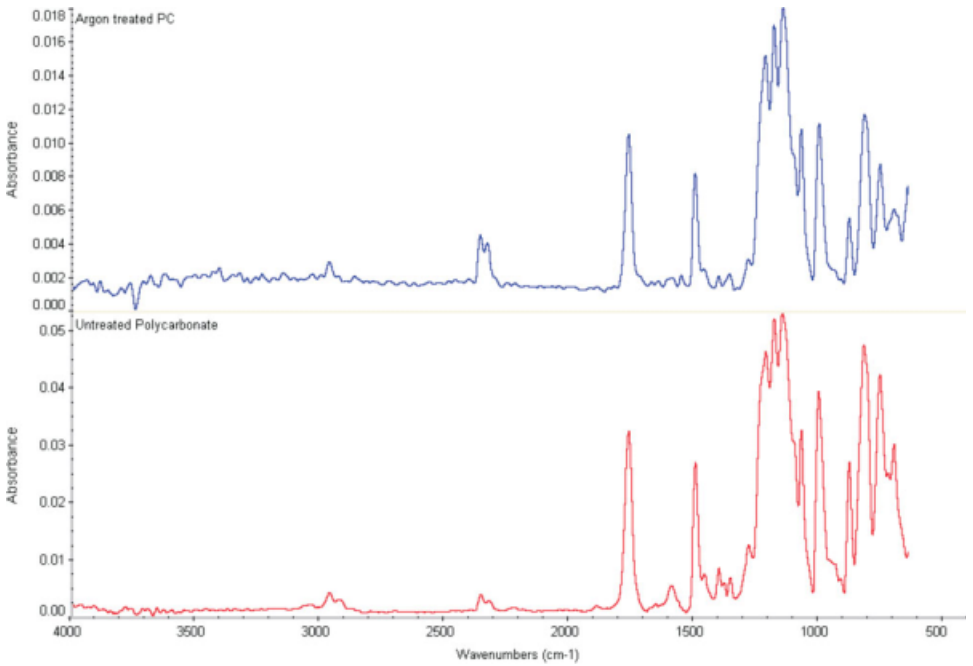

Figure 3 FTIR spectra of untreated and argon-plasma-treated polycarbonate. [Color figure can be viewed in the online issue, which is available at www.interscience.wiley.com.]

Surface chemistry of the polycarbonate

The analysis of polycarbonate with ATR–FTIR was of interest in connection with the structural modification of the polycarbonate that occurred due to plasma treatment. A great many of the changes in the molecular vibrations caused by the structural changes could be effectively studied by FTIR techniques. The FTIR spectra of the untreated and argon-plasma-treated polycarbonate are presented in Figure 3. The values of the relative absorbance [i.e., the ratio of the absorbance of the plasma-treated polycarbonate (A) to the absorbance of the untreated polycarbonate (A_0)] of various bands of polycarbonate are presented in Table III. The bands appearing at 706 cm^{-1} (out-of-plane bending mode of hydrogen attached to a phenyl ring), 763 cm^{-1} (out-of-plane skeletal vibration of C—H deformation), 1076 cm^{-1} and 1008 cm^{-1} (aromatic C—H deformation), and 1363 and 1408 cm^{-1} (C—H bending vibration of CH_3) showed a reduction in the absorbance after argon plasma treatment due to hydrogen abstraction. This led to the formation of free radicals, which

TABLE III
A/A_0 Values of the Identified Absorption Bands

Group	Wave number (cm^{-1})	A/A_0	Comment
Out-of-plane bending mode of hydrogen attached to the phenyl ring	706	0.20	Hydrogen abstraction
Out-of-plane skeletal vibration of C—H deformation	763	0.21	Hydrogen abstraction
C—O—C vibrational mode in ether	1220	0.55	Breakage of the ether group
	1154	0.34	
	1186	0.33	
Aromatic in-plane C—C stretching vibration	1598	0.37	Bond breaking at the benzene ring
	1502	0.31	
Characteristic bond of the polycarbonate corresponding to C=O stretching of the carbonyl	1769	0.33	Chain scission breaking C=O bonds
Aromatic CH deformation	1076	0.33	Hydrogen abstraction
	1008	0.28	
Asymmetrical CH stretching vibration of CH_3	2969	0.74	Cleavage of the methyl group
C—H bending vibration of CH_3	1363	0.32	Hydrogen abstraction
	1408	0.24	
Stretching vibration of C=C	1659	–	Double-bond formation
—OH	3419	–	Hydroxyl formation

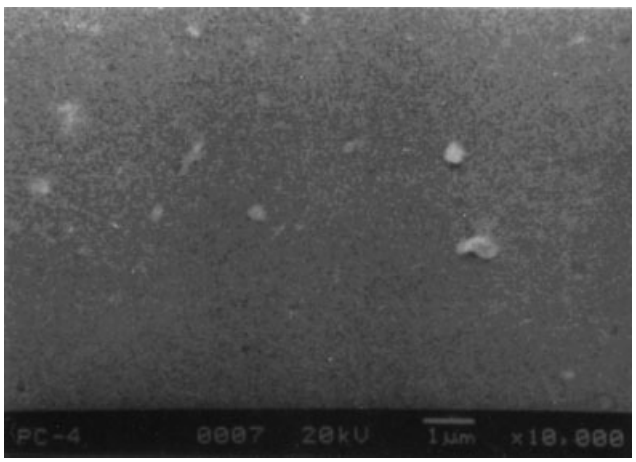

Figure 4 SEM picture of untreated polycarbonate.

then interacted to form crosslinked and unsaturated groups.[26] Double-bond formation by argon plasma etching and hydrogen abstraction were explained by the new peaks formed at 3047 cm^{-1} (=CH stretching vibration of alkenes) and 1659 cm^{-1} (C=C stretching vibration). Bond breaking at the benzene ring causing dearomatization was observed from the A/A_0 values of the peaks at 1598 and 1502 cm^{-1}, which corresponded to aromatic in-plane C—C stretching vibration. The breakage of the ether group, a skeleton of the macromolecule in the polycarbonate film, was indicated by the reduced absorbance value of the peaks corresponding to the ether groups at 1220, 1154, and 1186 cm^{-1}. Wang et al.[27] reported a decreased molecular weight due to the breakage of ether by argon ions. The chain scission that took place at the carbonate site broke C=O bonds and caused the reduction in their absorbance value. The breakage of C=O bonds and their removal in the form of CO or CO_2 have been reported for the irradiation of polycarbonate by various species. The new peak formed at 3419 cm^{-1}, attributed to the —OH group, indicated —OH group formation after hydrogen abstraction and the cleavage of carbonate linkages.[7] The importance of bond dissociation by argon plasma can be summarized on the basis of the relative intensities in the following order: (1) hydrogen abstraction, (2) carbonate cleavage, (3) dearomatization, and (4) breakage of the ether group.

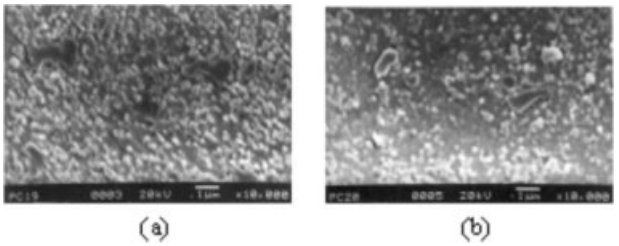

Figure 6 SEM pictures of polycarbonate treated at 110 W and 15 sccm for 6 min at pressures of (a) 200 and (b) 100 mTorr.

SEM

An SEM picture of the untreated polycarbonate given in Figure 4 clearly indicates the surface nature of the polymer. The argon-plasma-treated polycarbonate showed increased roughness, as shown in Figures 5–8. Plasma etching caused by the impact of the active species on the polymer surface increased its roughness. The etching of polycarbonate by argon plasma depended on the ion density and ion energy, which were influenced by RF power. The energy distribution of ions bombarding the substrate was governed by RF power.[28–30] The substrate was found to be more etched at 200 W than at 20 W, as shown in Figure 5. Similarly, at a pressure of 200 mTorr, the samples exhibited a more enhanced roughness, as shown in Figure 6, than at the lower pressure of 100 mTorr. This was probably because of the intense etching by more active species in plasma with a high density on the polymer surface.[31] The surface roughness was more pronounced at a lower flow rate of argon gas (Fig. 7). This may have been due to the property of a large number of charged species as a result of the better ionization of argon gas at a lower flow rate. A similar type of behavior was studied by Carrino et al.[19] as an interaction effect of

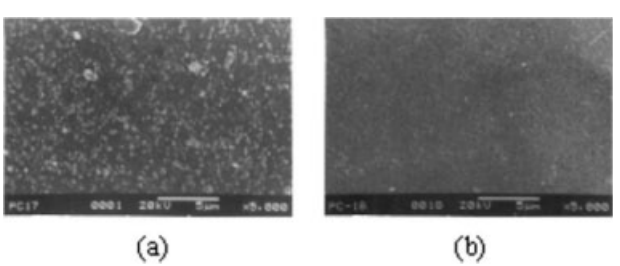

Figure 5 SEM pictures of polycarbonate treated at 150 mTorr and 15 sccm for 6 min at powers of (a) 200 and (b) 20 W.

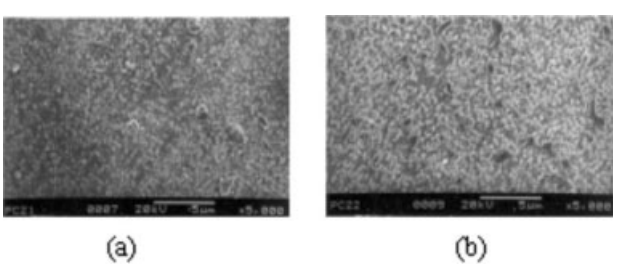

Figure 7 SEM pictures of polycarbonate treated at 110 W and 150 mTorr for 6 min at flow rates of (a) 20 and (b) 10 sccm.

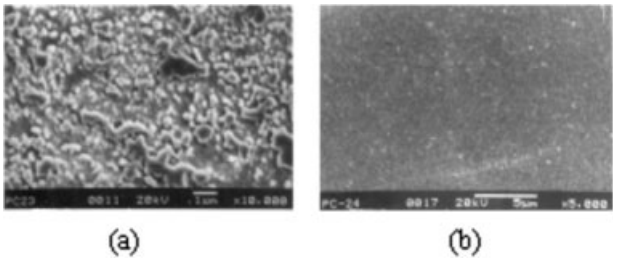

Figure 8 SEM pictures of polycarbonate treated at 110 W, 150 mTorr, and 15 sccm for treatment time (a) 10 and (b) 2 min.

the flow rate and voltage. The effect of time was easily understood by the fact that more etching of the polymers by the active species took place with longer exposure to the plasma (Fig. 8).

AFM

The surface morphology of a material treated by plasma is greatly influenced by the plasma treatment conditions along with the type and characteristics of the initiating gases.[32] The surface morphology of the polycarbonate at two levels of power was surveyed. An increase in the surface roughness was evident from the AFM images of the untreated and treated polycarbonates, as presented in Figure 9. The pristine polycarbonate surface was relatively smooth, which was indicated by both the AFM image [Fig. 9(a)] and the root-mean-square surface roughness of 37.31 nm. After plasma treatment, the roughness was enhanced significantly, which is more pronounced at high power (210.04 nm) than at low power (72.76 nm). The effect of plasma bombardment at various RF power levels with increasing root-mean-square roughness of the polycarbonate substrates explained the results of the contact angle measurements. This result was in agreement with the findings reported by Kang et al.[33] at various RF power levels in the plasma treatment of polycarbonate and poly(ether sulfone). The appearance of small grains on the surface of the polycarbonate after plasma treatment was reported and found to increase with the intensity of the plasma.[34] A greater number of grains were formed when the polycarbonate was treated at higher power, as shown in Figure 9(a,b). The peak-to-peak distances of the treated polycarbonate at 200 W (1215 nm/μm) and 20 W (525.6 nm/μm) were also observed to be greater than that of the untreated polycarbonate (354.9 nm/μm), and also, the treated surface was more uniform.

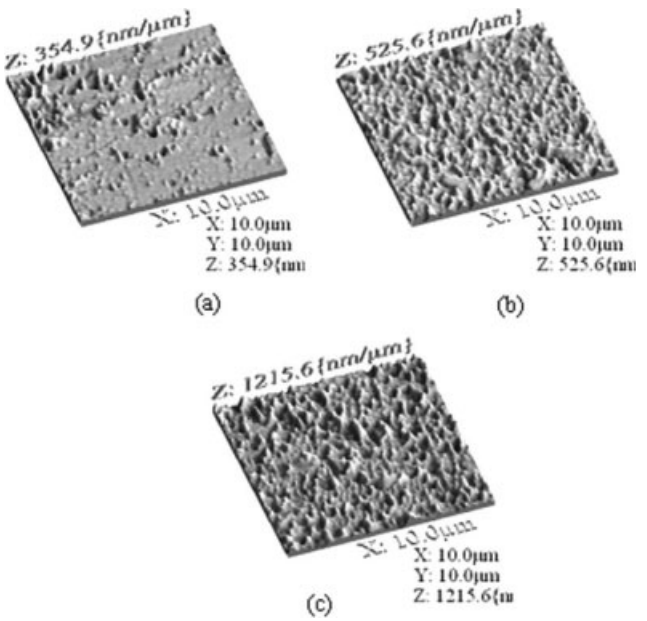

Figure 9 AFM images of (a) untreated polycarbonate and (b,c) polycarbonate treated at 150 mTorr and 15 sccm for 6 min at powers of 20 and 200 W, respectively.

TABLE IV
Estimated Regression Coefficients and Corresponding *P* Values for the Surface Energy of the Polycarbonate

Model term	Coefficient estimate	Standard error	*P* value
Intercept	38.98	0.26	–
X_1	−1.19	0.13	<0.0001
X_2	1.43	0.13	<0.0001
X_3	0.24	0.13	0.0907
X_4	2.232×10^{-3}	0.13	0.9867
X_1X_2	0.02	0.16	0.9057
X_1X_3	0.28	0.16	0.1027
X_1X_4	−0.35	0.16	0.0476
X_2X_3	−0.26	0.16	0.1348
X_2X_4	−0.31	0.16	0.0713
X_3X_4	0.16	0.16	0.3338
X_1^2	−0.083	0.12	0.5134
X_2^2	−0.39	0.12	0.0069
X_3^2	−0.19	0.12	0.1415
X_4^2	0.21	0.12	0.1132

Effect of the treatment conditions

Table II presents the experimental conditions and data resulting from the investigation of the effects of

TABLE V
ANOVA Results for the Quadratic Equation for the Surface Angle of the Polycarbonate

Source	Sum of squares	Degrees of freedom	Mean square	*F*	*P*
Model	97.64	14	6.97	16.63	<0.0001
Residual	6.29	15	0.42		
Lack of fit	2.74	10	0.27	0.39	0.9061
Pure error	3.55	5	0.71		

Standard deviation = 2.24; R^2 = 0.9395; adjusted R^2 = 0.8830; predicted R^2 = 0.7989; CV = 1.68%.

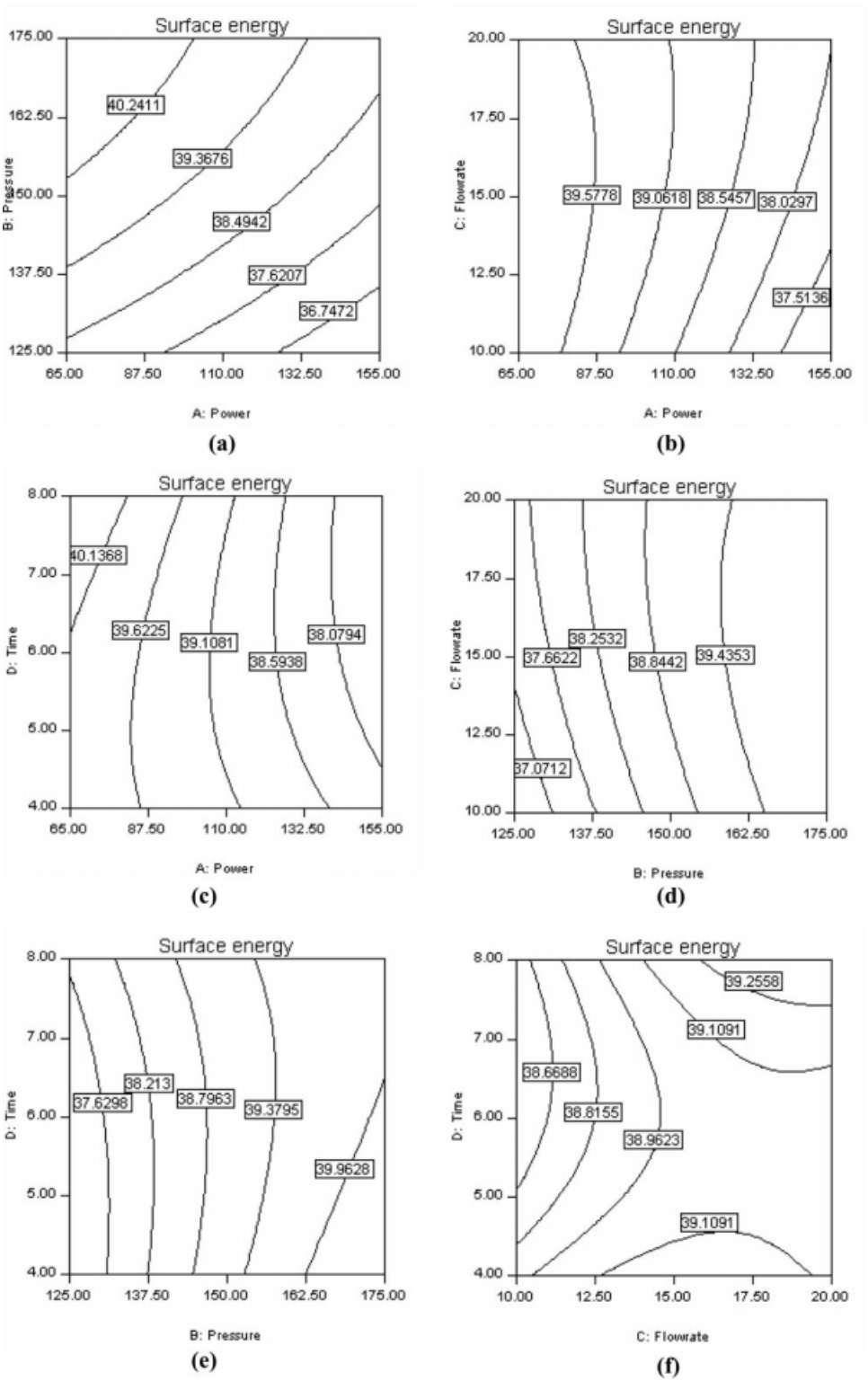

Figure 10 Contour plots of the surface energy plotted for (a) the power and pressure, (b) the power and flow rate, (c) the power and treatment time, (d) the pressure and flow rate, (e) the pressure and treatment time, and (f) the flow rate and time. The other variables were held at the following values: power = 110 W, pressure = 150 mTorr, flow rate = 15 sccm, and time = 6.00 min.

four variables (the RF power, pressure, flow rate of argon gas, and plasma treatment time) on the surface energy.

The data in Table II were run through RSM to construct an empirical model for the representation of the surface energy in terms of four independent

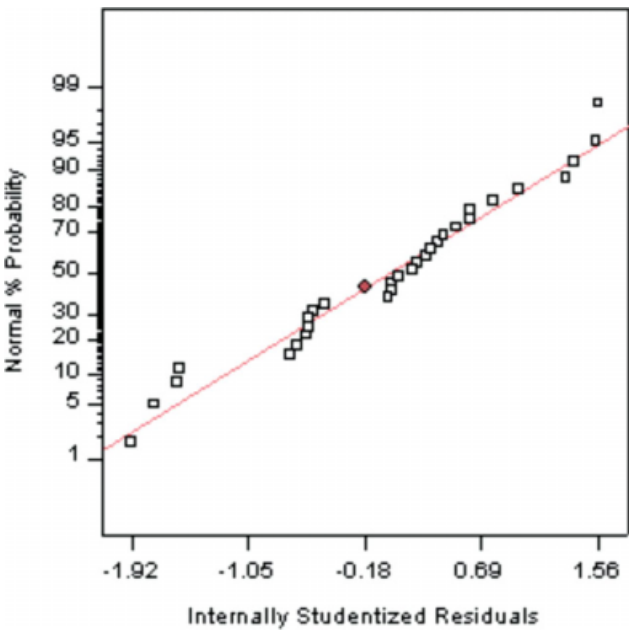

Figure 11 Normal plot of residuals. [Color figure can be viewed in the online issue, which is available at www.interscience.wiley.com.]

variables. On the basis of a regression analysis at a 95% confidence interval, the P values of the parameter estimations were found to be significant. The quadratic model was used to fit the observed data by least-square analysis. The coefficients of regression were computed with Design Expert, and the following regression equation was obtained:

$$\begin{aligned} Y = {} & 9.29149 - 0.015543 \times X_1 + 0.30947 \times X_2 \\ & + 0.35056 \times X_3 + 0.50419 \times X_4 + 1.73355 \times 10^{-5} \\ & \times X_1 \times X_2 + 1.25049 \times 10^{-3} \times X_1 \times X_3 - 3.88117 \\ & \times 10^{-3} \times X_1 \times X_4 - 2.04712 \times 10^{-3} \times X_2 \times X_3 \\ & - 6.28511 \times 10^{-3} \times X_2 \times X_4 + 0.016169 \times X_3 \times X_4 \\ & - 4.08737 \times 10^{-5} \times X_1^2 - 6.19261 \times 10^{-4} \times X_2^2 \\ & - 7.67503 \times 10^{-3} \times X_3^2 + 0.052008 \times X_4^2 \end{aligned} \quad (2)$$

where X_1 is the RF power, X_2 is the pressure, X_3 is the flow rate of argon gas, and X_4 is the plasma treatment time. The significance of each coefficient was inferred from the P values, which are presented in Table IV. The power had a significant negative linear effect on the surface energy ($P < 0.0001$), whereas the pressure displayed a positive effect ($P < 0.0001$). Significant interactions were observed between power and time. Quadratic effects of pressure also showed significant effects on the surface energy.

The ANOVA results of the quadratic regression model presented in Table V indicates that the model equation adequately described the response surface of the surface energy in the interval of investigation, as was evident from the F test ($F = 16.63$) with a low P value [(model $P_1 > F$) < 0.0001]. The goodness of fit of this model was explained by the R^2 value of 0.9395, with only 6.05% of the total variations in the data being not explained. This model was also robust because the predicted R^2 (0.7989) was in reasonable agreement with the adjusted R^2 (0.8830). A lower value of the coefficient of variation (CV; 1.68%) showed that the experiments conducted were precise and reliable.[35] The larger Fisher's t values with lower P values indicated statistical significance of the estimated regression coefficients.[14]

Process optimization

Figures 10(a–f) represent the contour plots for the optimization of the process conditions of the surface energy. Each figure presents the effect of two variables on the surface energy of the polycarbonate, whereas the other two variables were held at zero level. An elliptical contour plot indicated a significant interaction between the respective variables, whereas the circular contour plot is an indication of insignificant interaction of the related variables. From the contour plots, the surface energy, approximately in the range of 40 mN/m was observed to lie in the following range of process variables: power = 65–135 W, pressure = 150–175 mTorr, flow rate = 10–20 sccm, and treatment time = 4–8 min. Solving the quadratic model on the basis of the data obtained from Table II revealed that an optimum response (surface energy = 41.5491 mN/m) was achieved with a desirability of 0.98 under process conditions of 65 W, 175 mTorr, 10.21 sccm, and 4 min.

Model adequacy and validation of the model

To ensure the adequate approximation of a model to the real system, the model adequacy should be checked. By constructing a normal probability plot of the residuals, we made a check for the normality assumption (Fig. 11). The plot indicated that the normality assumption was satisfied, as the residuals plotted were approximated along a straight line.[20]

A comparison of the predicted optimized surface energy with the experiment conducted under the predicted optimal conditions of the process factors (power = 65 W, pressure = 175 mTorr, flow rate = 10 sccm, and treatment time = 4 min) confirmed the optimization results. This optimized process conditions yielded a polymer surface energy of

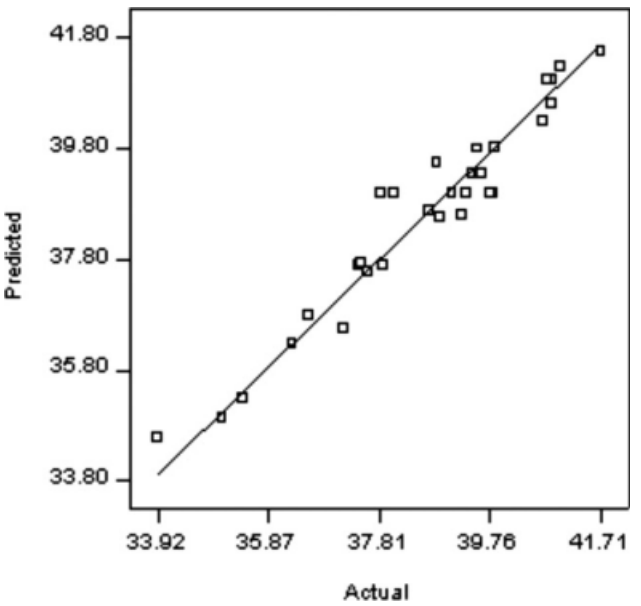

Figure 12 Predicted surface energy versus the actual surface energy.

41.71 mN/m, which was closer to the predicted surface energy (41.55 mN/m) under the same optimal conditions. The error between the predicted and actual surface energy was found to be 0.38%, which was quite low. In addition, a high level of similarity between the predicted and observed results, shown in the plot of predicted versus actual surface energy, indicated the accuracy of the statistical model (Fig. 12).

CONCLUSIONS

The wettability studies showed that the surface energy increased in all conditions after plasma surface treatment, which meant that the hydrophilicity was improved. The SEM and AFM results supported the increased surface energy results by exhibiting increased roughness. A quadratic model was developed with terms of power, pressure, flow rate, and time to represent the surface energy with RSM of a central composite design. The response evaluated from the quadratic model showed good agreement with the observed ones. We optimized the process conditions from the predicted model and confirmed them by running the experiment under the predicted optimum conditions. The prediction accuracy of the model was found to be very high.

The authors gratefully acknowledge Prof. S. Dasgupta (Department of Chemical Engineering, Indian Institute of Technology, Kharagpur, India) for providing the contact-angle-measurement facilities.

References

1. Vallon, S.; Hofrichter, A.; Guyot, L.; Drevillon, B.; Klemberg-Sapieha, J. E.; Martinu, L.; Poncin-Epaillard, F. J Adhes Sci Technol 1996, 10, 1287.
2. Liston, E. M.; Martinu, L.; Wertheimer, M. R. In Plasma Surface Modification of Polymers; Strobel, M.; Lyons, C.; Mittal, K. L., Eds.; VSP: Utrecht, The Netherlands, 1994; p 3.
3. Fakes, D. W.; Davies, M. C.; Brown, A.; Newton, J. M. Surf Interface Anal 1998, 13, 233.
4. Lee, J. H.; Park, J. W.; Lee, H. B. Biomaterials 1991, 12, 443.
5. Hettlich, H.-J.; Otterbach, F.; Mittermayer, C.; Kaufmann, R.; Klee, D. Biomaterials 1991, 12, 521.
6. Sterrett, T. L.; Sachdeva, R.; Jerabek, P. J Mater Sci: Mater Med 1992, 3, 402.
7. Zajickova, L.; Subedi, D. P.; Bursikova, V.; Veltruska, K. Acta Phys Slov 2003, 53, 489.
8. Grant, J. L.; Dunn, D. S.; McClure, D. J. J Vac Sci Technol A 1988, 6, 2213.
9. Schonhorn, H.; Hansen, R. H. J Appl Polym Sci 1967, 11, 1461.
10. Kwon, O.-J.; Tang, S.; Myung, S.-W.; Lu, N.; Choi, H.-S. Surf Coat Technol 2005, 192, 1.
11. Francis, F.; Sabu, A.; Madhavan, K. N.; Sumitra, R.; Sanjoy, G.; George, S.; Pandey, A. Biochem Eng J 2003, 15, 107.
12. Gomathi, N.; Venkata Prasad, K.; Neogi, S. J Appl Polym Sci 2009, 111, 1917.
13. Gomathi, N.; Neogi, S. Appl Surf Sci 2009, 255, 7590.
14. Bhat, N. V.; Upadhyay, D. J.; Deshmukh, R. R.; Gupta, S. K. J Phys Chem B 2003, 107, 4550.
15. Pandiyaraj, K. N.; Selvarajan, V.; Deshmukh, R. R.; Changyou, G. Vacuum 2009, 83, 332.
16. Grill, A. Cold Plasma in Materials Fabrication from Fundamental to Applications; IEEE: New York, 1993.
17. Carrino, L.; Moroni, G.; Polini, W. J Mater Process Technol 2002, 121, 373.
18. Carrino, L.; Polini, W.; Sorrentino, L. J Mater Process Technol 2004, 153, 519.
19. Myers, R. H.; Montgomery, D. C. Response Surface Methodology; Wiley: New York, 2002.
20. Rajesh, D.; Mark, J. K. J Phys D 2000, 36, 666.
21. Wheale, S. H.; Barker, C. P.; Badyal, J. P. S. Langmuir 1998, 14, 6699.
22. Wrobel, A. M.; Kryszewski, M.; Rakowski, W.; Okoniewski, M.; Kubacki, Z. Polymer 1978, 19, 908.
23. Rockova, K.; Svorcık, V.; Bacakova, L.; Dvorankova, B.; Hnatowicz, V. Nucl Instrum Methods B 2004, 225, 275.
24. Harth, K.; Hibst, H. Surf Coat Technol 1993, 59, 350.
25. Chan, C.-M.; Ko, T.-M.; Hiraoka, H. Surf Sci Rep 1996, 24, 1.
26. Wang, Y.; Jin, Y.; Zhu, Z.; Liu, C.; Sun, Y.; Wang, Z.; Hou, M.; Chen, X.; Zhang, C.; Liu, J.; Li, B. Nucl Instrum Methods Phys Res B 2000, 164, 420.
27. Godyak, V. A.; Piejak, R. B.; Alexandrovich, B. M. Plasma Sources Sci Technol 1992, 1, 36.
28. Kawamura, E.; Vahedi, V.; Lieberman, M. A.; Birdsall, C. K. Plasma Sources Sci Technol 1999, 8, R45.
29. Zajıckova, L.; Bursıkova, V.; Perina, V.; Mackova, A.; Subedi, D.; Janca, J.; Smirnov, S. Surf Coat Technol 2001, 142, 449.
30. Collaud, M.; Nowak, S.; Kuttel, O. M.; Groning, P.; Schlapbach, L. Appl Surf Sci 1993, 72, 19.
31. Coen, M. C.; Dietler, G.; Kasas, S.; Groning, P. Appl Surf Sci 1997, 103, 99.
32. Kang, S. M.; Yoon, S. G.; Yoon, D. H. Thin Solid Films 2008, 516, 1405.
33. Larsson, A.; Derand, H. J Colloid Interface Sci 2002, 246, 214.
34. Box, G. E. P.; Hunter, W. G.; Hunter, J. S. Statistics for Experimenters; Wiley: New York, 1978.
35. Sharma, D. C.; Satyanarayan, T. Bioresour Technol 2006, 97, 727.